



HAL
open science

The spectral functions method for acoustic wave diffraction by a stress-free wedge: Theory and validation

Samar Chehade, Audrey Kamta Djakou, Michel Darmon, Gilles Lebeau

► To cite this version:

Samar Chehade, Audrey Kamta Djakou, Michel Darmon, Gilles Lebeau. The spectral functions method for acoustic wave diffraction by a stress-free wedge: Theory and validation. *Journal of Computational Physics*, 2019, 377, pp.200-218. 10.1016/j.jcp.2018.10.040 . cea-04432546

HAL Id: cea-04432546

<https://cea.hal.science/cea-04432546>

Submitted on 1 Feb 2024

HAL is a multi-disciplinary open access archive for the deposit and dissemination of scientific research documents, whether they are published or not. The documents may come from teaching and research institutions in France or abroad, or from public or private research centers.

L'archive ouverte pluridisciplinaire **HAL**, est destinée au dépôt et à la diffusion de documents scientifiques de niveau recherche, publiés ou non, émanant des établissements d'enseignement et de recherche français ou étrangers, des laboratoires publics ou privés.

The spectral functions method for acoustic wave diffraction by a stress-free wedge : theory and validation

Samar **Chehade**^{a,*}, Audrey **Kamta Djakou**^a, Michel **Darmon**^a, Gilles **Lebeau**^b

^aCEA LIST, Department of Imaging & Simulation for Nondestructive Testing, CEA-Saclay, DIGITEO LABs, bat 565, 91191 Gif-sur-Yvette, France

^bLaboratoire J.A. Dieudonné, UMR CNRS 7351, Université de Nice Sophia-Antipolis, Parc Valrose, 06108 NICE, France

Non Destructive Examination (NDE) of industrial structures requires the modeling of specimen geometry echoes generated by the surfaces (entry, backwall ...) of inspected blocks. For that purpose, the study of plane wave diffraction by a wedge is of great interest. The work presented here is preliminary research to model the case of an elastic wave diffracted by a wedge in the future, for which there exist various modeling approaches but the numerical aspects have only been developed for wedge angles lower than π . The spectral functions method has previously been introduced to solve the 2D diffraction problem of an immersed elastic wedge for angles lower than π . As a first step, the spectral functions method has been developed here for the diffraction on an acoustic wave by a stress-free wedge, in 2D and for any wedge angle, before studying the elastic wave diffraction from a wedge. In this method, the solution to the diffraction problem is expressed in terms of two unknown functions called the spectral functions. These functions are computed semi-analytically, meaning that they are the sum of two terms. One of them is determined exactly and the other is approached numerically, using a collocation method. A successful numerical validation of the method for all wedge angles is proposed, by comparison with the GTD (Geometrical Theory of Diffraction) solution derived from the exact Sommerfeld integral.

1. Introduction

The canonical problem of an acoustic, electromagnetic or elastodynamic plane wave diffraction by a wedge with Neumann or Dirichlet boundary conditions is a complex mathematical problem which has been of great interest to researchers for over a century.

*Corresponding author: Tel.: +33-1-69-08-34-26;

e-mail: samar.chehade@cea.fr (Samar Chehade), michel.darmon@cea.fr (Michel Darmon)

The mathematical theory of wedge diffraction was first introduced by Sommerfeld [1], who gave an analytical expression of the exact solution of the diffraction problem of a scalar plane wave as a contour integral [2]. Macdonald [3] has expressed the scalar solution as a series, using the variables separation technique.

The most common approximation of diffraction problems is that of far-field asymptotics (i.e. wave behavior when $kr \gg 1$, k being the wave number and r the observation distance). The Geometrical Theory of Diffraction (GTD) was first proposed by Keller [4] in electromagnetics based on an asymptotic expansion of Sommerfeld's exact solution. Sommerfeld [1] gave an analytical formula of the GTD diffraction coefficient for an arbitrary-angled wedge (with Neumann or Dirichlet boundary conditions) illuminated by a scalar plane wave. This wedge GTD coefficient can be used for scalar wave diffraction both in electromagnetics [5] and in acoustics [6, 7].

In the more complex case of an elastic wave diffracted by a wedge of angle less than π , there exist two major approaches : one is based on the Sommerfeld integral (SI) representation of the elastodynamic potentials, it was introduced by Budaev and Bogy [8] and clarified by Kamotski et al. [9]. The other method is based on the Laplace transform of the displacement field (LT), and was developed by Gutesen and Fradkin [10]. In the particular case of a scattered Rayleigh wave, a method which uses the free-space Green's tensor to express the Fourier transform of the displacement field has been developed by Gutesen for wedge angles smaller and greater than π [11, 12]. However the range of the wedge angle was restricted to the range $[63^\circ, 180^\circ]$ for angles smaller than π and to $[189^\circ, 327^\circ]$ for angles greater than π in order to avoid numerical instabilities.

These methods are non-uniform in the sense that they lead to a solution which diverges at shadow boundaries and caustics of the Geometric-Elastic (GE) field [6]. To overcome this difficulty, Ufimtsev [13] has introduced the Physical Theory of Diffraction (PTD) in electromagnetics. This technique has been extended to elastic waves by Zernov et al. [14], however it is computationally expensive. Another uniform correction of GTD is the Uniform Asymptotic Theory (UAT), introduced by Lewis [15] in electromagnetics and acoustics and extended to elastodynamics by Achenbach et al. [16], which gives a systematic approach for computing a uniform solution but is quite complicated to implement for complex geometries as it requires extension of the reflected field to its shadow zone using fictitious rays [6], [17]. For practical purposes, the most used uniform correction of the GTD method is the Uniform Theory of Diffraction (UTD) as it is computationally efficient and does not require an artificial extension of the reflected field. It was developed in electromagnetics by Kouyoumjian and Pathak [5], using the Pauli-Clemmow method [18] and extended to elastodynamics by Kamta Djakou et al. [19]. A comparison of different asymptotic (GTD and uniform) and exact solutions has been carried out in elastodynamics by Aristizabal et al. [20] but for the scalar case of the 2D wedge diffraction of a shear horizontally polarized incident wave.

For a certain time, methods of computation have been studied without proof of solvability for the wedge diffraction problem. Osher [21, 22] has studied the well-posedness of hyperbolic initial and boundary value problems (meaning the solution is fixed at $t = 0$ and on the domain boundaries) in a region with a corner (meaning a right-angled wedge) and has given certain necessary conditions that the boundary values must verify in order for a problem to be well-posed; he has thoroughly presented the consequences if these conditions were not verified. Huang and Temam [23] have studied the well-posedness of hyperbolic initial and boundary value problems in a rectangular domain and have also specified how the boundary values must be chosen for the problem to be solvable; they have also given a brief explanation as to how their theory can be applied to wave equations.

Concerning the specific problem of wave propagation in a wedge-shaped region, Friedlander [24] has studied the problem in the case of an incident acoustic pulse (the incident wave is non-periodical in time) and constructed the corresponding Green's function. Castro and Kapanadze [25] have proven existence and uniqueness of the solution for acoustic and electromagnetic plane waves using a detailed Fredholm analysis. Kamotski and Lebeau [26] have proven existence and uniqueness of the solution to the elastic plane wave diffraction by a soft wedge (Dirichlet boundary) problem using the Spectral Functions method in which the diffracted wave is modeled thanks to these spectral functions. Their demonstration is valid for all wedge angles but they do not propose any method of computation of the solution. The Spectral Functions method was at first developed by Croisille and Lebeau [27] who proposed a numerical algorithm in order to compute these functions for elastic wedges of angle lower than π immersed in a fluid. In the current paper, wedges of any angle (even larger than π) are taken into account, and the outside medium is void. There is only one wave type to be considered and Dirichlet boundary conditions are supposed, as opposed to the case studied by Croisille and Lebeau [27] where three propagation modes coupled by the boundary conditions are considered, but only for wedge angles lower than π .

In the field of seismic diffraction, other approaches have been developed. The problem of acoustic diffraction in a system of wedge-shaped regions was studied by Klem-Musatov [28]. Using the Maluzhinetz transform, this

problem is reduced to a system of functional equations. However, this system is too complex to be solved in general cases. A successive approximations method is proposed in the particular case of a wedge-shaped separation between two media having the same acoustic wave velocity or in the case where the medium containing the incident wave is a wedge of angle lower than π . In the very general case of acoustic wave propagation in a homogeneous or inhomogeneous medium delimited by an arbitrary-shaped boundary, a mathematical model has been rigorously presented by Aizenberg and Ayzenberg [29], providing the analytical feasible fundamental solution for this problem. The notion of feasible fundamental solution is a generalization of Green's function for an unbounded medium. Ayzenberg [30] shows how this general mathematical model can be numerically applied to the case of wedge diffraction. This method is applied in the case of a spherical source and it appears that parallel computation is necessary to obtain a short computation time, whereas the spectral functions method is applied here in the case of plane-wave diffraction and a simple architecture is sufficient to obtain results for a short computation time.

The aim of this paper is to develop and implement the methodology of Croisille and Lebeau [27] in the two-dimensional (i.e. the incident wave vector lies in the plane normal to the edge) case of an acoustic wave diffracted by a soft wedge immersed in a fluid (Dirichlet boundary condition) and propose a numerical validation of the method for angles both smaller and larger than π . The expansion to all wedge angles is obtained using Kamotski and Lebeau's [26] idea of defining a new angular variable, 2φ , defined in equation (28), thanks to which the complete resolution and the computation of the solution are proposed and developed here for all wedge angles with a single method. Numerical validation will be achieved by comparing the GTD approximation of the diffraction coefficient obtained using the spectral functions method, with the analytical expression given in [6, 7] of the GTD approximation of the exact solution.

The outline of the paper is the following: section 2. presents the problem and the diffraction coefficients are expressed in terms of the spectral functions. The resolution of the problem is discussed in section 3. Finally, numerical results are given in section 4. and compared to the analytical Sommerfeld solution.

2. Problem statement

Let us consider a stress-free wedge of angle 2φ immersed in a fluid Ω_f constituted of the junction of two faces F_1 and F_2 (see Fig. 1). The Cartesian coordinate system $(O; \mathbf{e}_{x_1}, \mathbf{e}_{y_1})$ is linked to the face F_1 of the wedge and $(O; \mathbf{e}_{x_2}, \mathbf{e}_{y_2})$ is linked to the face F_2 . These Cartesian coordinate systems have the same origin located on the wedge edge which coincides with the z -axis. Let $\mathbf{x} = (x_1, y_1)_{(\mathbf{e}_{x_1}, \mathbf{e}_{y_1})} = (x_2, y_2)_{(\mathbf{e}_{x_2}, \mathbf{e}_{y_2})}$ be a position vector $\mathbf{x} = (r, \theta)$ in a local basis of polar coordinates associated to the Cartesian coordinates (x_1, y_1) . The time convention used in this chapter is $\exp(i\omega t)$. The wedge is thus irradiated by a velocity potential plane wave in the form

$$g^{\text{inc}}(\mathbf{x}, t) = A e^{i(\omega t - \mathbf{k}^{\text{inc}} \cdot \mathbf{x})} \quad (1)$$

where A is the amplitude of the incident velocity potential, ω is the circular frequency, t is time and

$$\mathbf{k}^{\text{inc}} = k_0(-\cos \theta_{\text{inc}}, -\sin \theta_{\text{inc}})_{(\mathbf{e}_{x_1}, \mathbf{e}_{y_1})} \quad (2)$$

is the wave vector of the incident wave with $k_0 = \omega/c_0$ being the wave number - c_0 is the sound velocity in the fluid. The velocity potential in the fluid g satisfies the motion equation in the fluid medium Ω_f surrounding the wedge

$$\frac{\partial^2 g}{\partial t^2} - c_0^2 \Delta g = 0 \quad (3)$$

and the Dirichlet boundary condition on the wedges faces

$$g|_{F_j} = 0, \quad j = 1, 2. \quad (4)$$

The dimensionless form of the problem is obtained by defining the function h by

$$g(\mathbf{x}, t) = 2A e^{i\omega t} h(k_0 \mathbf{x}). \quad (5)$$

The dimensionless function h is the sum of the incident dimensionless wave h_{inc} and of the scattered dimensionless wave v

$$h = h_{\text{inc}} + v \quad (6)$$

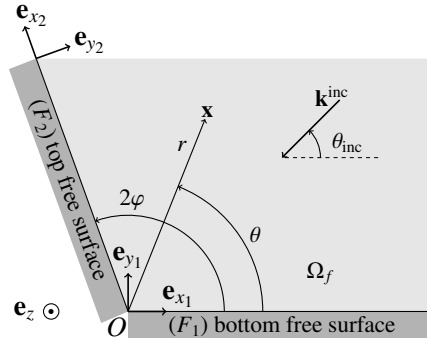


Fig. 1: The wedge of angle 2φ whose faces are stress-free is illuminated by a plane wave of wave vector \mathbf{k}^{inc} .

In this decomposition, the scattered wave v is the sum of two fields : the Geometric-Elastodynamic (GE) field, which is the sum of the possibly multiple specular reflections of the incident wave and of fictitious fields compensating the incident wave in shadow zones, and the diffracted field. A detailed description of the GE field, in the case of a half-plane scatterer, is given by Kamta-Djakou et al. [19].

The system (3)-(4) is equivalent to the following system of equations for the dimensionless problem, obtained by inserting Fourier transform (5) and decomposition (6) into equations (3) and (4)

$$\begin{cases} (\Delta + 1)v = 0 & \text{in } \Omega_f, \\ v = -h_{\text{inc}} & \text{on } F_j, \quad j = 1, 2 \end{cases} \quad (7)$$

In order to obtain a solution to this problem which is physically relevant, the limiting absorption principle is used. It consists in substituting the wave number k_0 by a complex one $k_0 e^{-i\epsilon}$ with $\epsilon > 0$. This means that absorption occurs in the medium and thus the scattered waves attenuate with the distance. The system (7) then becomes :

$$(S_\epsilon^*) \quad \begin{cases} (\Delta + e^{-2i\epsilon})v^\epsilon = 0 & \text{in } \Omega_f, \\ v^\epsilon = -h_{\text{inc}}^\epsilon & \text{on } F_j, \quad j = 1, 2 \end{cases} \quad (8)$$

The physically relevant solution to (7), called the outgoing solution, can now be defined. It is the one obtained when taking $\epsilon \rightarrow 0$ in (8). This limit is noted v^0 . Its integral representation is found hereafter.

Outgoing solution: integral representation

First, a special class of distributions is defined.

Definition 2.1. The class of distributions \mathcal{A} is defined as follows. The distribution $f \in \mathcal{A}$ if :

- $f \in \mathcal{L}^2(\mathbb{R})$ (f is a tempered distribution)
- $\text{supp}(f) \subset [0, +\infty[$
- $\exists C_0 > 0$ such that

$$\sup_{-\pi < \theta < 0} \int_{\rho > C_0} |\hat{f}(\rho e^{i\theta})|^2 d\rho < \infty$$

where \hat{f} is the Fourier transform of f defined by $\hat{f}(\xi) = \int_{\mathbb{R}} f(x) e^{-ix\xi} dx$.

- $\hat{f}(\xi)$ is holomorphic near $\xi = 1$

The outgoing solution to (7) can now be defined properly.

Definition 2.2. An outgoing solution of the equation (7) is a solution v of the form

$$v = v_1|_{\Omega_f} + v_2|_{\Omega_f} \quad (9)$$

where, for $j = 1, 2$:

$$v_j = -\lim_{\epsilon \rightarrow 0} (\Delta + e^{-2i\epsilon})^{-1} [\alpha_j \otimes \delta_{F_j}] \tag{10}$$

with $\alpha_j \in \mathcal{A}$ are unknown and where δ_{F_1} and δ_{F_2} are Dirac delta functions on the faces F_1 and F_2 of the wedge respectively (these functions take value $\delta_{F_j}(x, y) = 1$ on F_j , and 0 elsewhere).

The following theorem is proven by Croisille and Lebeau in [27] :

Theorem 2.1. *The equation (7) admits a unique outgoing solution.*

The aim of this paper is to extend and detail the computation of this outgoing solution for the stress-free wedge immersed in a fluid using the spectral functions method.

The double Fourier transform of a tempered distribution and its inverse are defined by :

$$\hat{f}(\xi, \eta) = \int \int_{\mathbb{R}^2} f(x, y) e^{-i(x\xi + y\eta)} dx dy \tag{11a}$$

$$f(x, y) = \frac{1}{4\pi^2} \int \int_{\mathbb{R}^2} \hat{f}(\xi, \eta) e^{i(x\xi + y\eta)} d\xi d\eta \tag{11b}$$

The double Fourier transform of (10) using (11a) gives

$$\hat{v}_j^\epsilon = [\xi^2 + \eta^2 - e^{-2i\epsilon}]^{-1} \hat{\alpha}_j. \tag{12}$$

The dimensionless velocity potential v_j^ϵ is then found by applying the inverse Fourier transform in ξ and η to (12).

$$v_j^\epsilon = \frac{1}{4\pi^2} \int_{-\infty}^{+\infty} \left(\int_{-\infty}^{+\infty} \frac{e^{iy_j\eta}}{\xi^2 + \eta^2 - e^{-2i\epsilon}} d\eta \right) \hat{\alpha}_j(\xi) e^{ix_j\xi} d\xi. \tag{13}$$

For $\epsilon \neq 0$, the inner integrand poles are given by

$$\eta = \pm \sqrt{e^{-2i\epsilon} - \xi^2} = \pm \zeta_0^\epsilon \tag{14}$$

and are never crossed by integration along the real axis. Integral (13) can be calculated using the residue theorem which leads to the following result

$$v_j^\epsilon(x_j, y_j) = \frac{i}{4\pi} \int_{-\infty}^{+\infty} \frac{e^{iy_j\zeta_0^\epsilon(\xi)} e^{ix_j\xi}}{\zeta_0^\epsilon(\xi)} \hat{\alpha}_j(\xi) d\xi. \tag{15}$$

This integral is well defined if $\text{Im}(\zeta_0^\epsilon) > 0$, so that the exponential in the integral decreases with the distance y_j and the absorption principle is respected. Function $\zeta_0^\epsilon(\xi)$ then satisfies for ξ real

$$\zeta_0^\epsilon(\xi) = i\sqrt{\xi^2 - e^{-i\epsilon}} \quad \text{if } |\xi| \geq 1, \tag{16a}$$

$$\zeta_0^\epsilon(\xi) = -\sqrt{e^{-i\epsilon} - \xi^2} \quad \text{if } |\xi| \leq 1. \tag{16b}$$

The branch points of the function $\zeta_0^\epsilon(\xi)$ are $\pm e^{-i\epsilon}$. For $\epsilon > 0$, integral (15) is well defined because these complex singular points are never crossed by the integration contour (the real axis). The integration contour of (15), is deformed into the contour Γ_0 illustrated on Fig. 2 so that these singular points $\pm e^{-i\epsilon}$ are not crossed by the new contour Γ_0 when $\epsilon \rightarrow 0$ (for which the physical outgoing solution of (8) is obtained). Arrows \mathcal{F}_1 and \mathcal{F}_2 on Fig. 2 are described later in section 3.2.2.

Thus, even for $\epsilon = 0$, the integral

$$v_j^0(x_j, y_j) = \frac{i}{4\pi} \int_{\Gamma_0} \frac{e^{iy_j\zeta_0^0(\xi)} e^{ix_j\xi}}{\zeta_0^0(\xi)} \hat{\alpha}_j(\xi) d\xi \tag{17}$$

converges. Using (9), our initial solution is then

$$v(\mathbf{x}) = v_1^0(x_1, y_1) + v_2^0(x_2, y_2) \tag{18}$$

One of the goals of this paper is to compute the spectral functions $\hat{\alpha}_1(\xi)$ and $\hat{\alpha}_2(\xi)$ in order to find the GTD diffraction coefficient (92). The accuracy of the spectral functions method is evaluated in section 4 by comparing results of (92) with (97). Section 3 is devoted to the computation of the spectral functions $\hat{\alpha}_1$ and $\hat{\alpha}_2$.

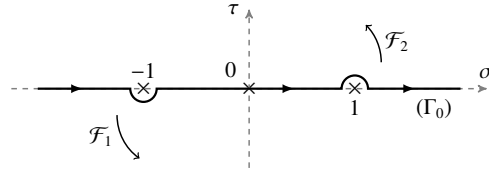


Fig. 2: Integration contour Γ_0 in the complex plane $\xi = \sigma + i\tau$. Arrows \mathcal{F}_1 and \mathcal{F}_2 show the deformation of Γ_0 into the imaginary axis.

3. Spectral functions computation

To compute the spectral functions, the functional equations satisfied by spectral functions $\hat{\alpha}_1$ and $\hat{\alpha}_2$ first have to be determined.

3.1. Functional equations of spectral functions

The velocity potential in the boundary conditions of the system (8) is substituted by its expression (18). It then leads to the following system of equations for the boundary conditions on each wedge face:

$$\begin{cases} v_1^0(x_1, 0) + v_2^0(x_2 \cos 2\varphi, x_2 \sin 2\varphi) = -v_{\text{inc}}^0 |_{F_1} \\ v_1^0(x_1 \cos 2\varphi, x_1 \sin 2\varphi) + v_2^0(x_2, 0) = -v_{\text{inc}}^0 |_{F_2} \end{cases} \quad (19)$$

The Fourier transform is applied to the potential velocity expression on the face of each wedge

$$\begin{aligned} \mathcal{F}(x_j \mapsto v_j^0(x_j, 0))(\xi) &= \frac{i}{4\pi} \int_{\Gamma_0} \frac{\hat{\alpha}_j(\lambda)}{\zeta_0^0(\lambda)} \left(\int_0^\infty e^{-ix_j(\xi-\lambda)} dx_j \right) d\lambda, \\ &= \frac{1}{4\pi} \int_{\Gamma_0} \frac{\hat{\alpha}_j(\lambda)}{\zeta_0^0(\lambda)(\xi - \lambda)} d\lambda \end{aligned} \quad (20)$$

and

$$\begin{aligned} \mathcal{F}(x_j \mapsto v_j^0(x_j \cos 2\varphi, x_j \sin 2\varphi))(\xi) &= \frac{i}{4\pi} \int_{\Gamma_0} \frac{\hat{\alpha}_j(\lambda)}{\zeta_0^0(\lambda)} \left(\int_0^\infty e^{-ix_j(\xi-\lambda \cos 2\varphi - |\sin 2\varphi| \zeta_0^0(\lambda))} dx_j \right) d\lambda, \\ &= \frac{1}{4\pi} \int_{\Gamma_0} \frac{\hat{\alpha}_j(\lambda)}{\zeta_0^0(\lambda) [\xi - \lambda \cos 2\varphi - |\sin 2\varphi| \zeta_0^0(\lambda)]} d\lambda. \end{aligned} \quad (21)$$

The dimensionless incident wave on the faces F_1 and F_2 of the wedge which is involved at the right side of (19) is respectively:

$$v_{\text{inc}}^0(x_1, 0) = \frac{1}{2} e^{ix_1 \cos \theta_{\text{inc}}}, \quad (22a)$$

$$v_{\text{inc}}^0(x_2, 0) = \frac{1}{2} e^{ix_2 \cos(2\varphi - \theta_{\text{inc}})}. \quad (22b)$$

Therefore, applying the Fourier transform to (19) leads to the following functional system of equations:

$$\begin{cases} DM(\hat{\alpha}_1)(\xi) + TM(\hat{\alpha}_2)(\xi) = \frac{1}{\xi - Z_1} \\ TM(\hat{\alpha}_1)(\xi) + DM(\hat{\alpha}_2)(\xi) = \frac{1}{\xi - Z_2} \end{cases} \quad (23)$$

where $Z_1 = \cos \theta_{\text{inc}}$, $Z_2 = \cos(2\varphi - \theta_{\text{inc}})$. DM is an integral operator defined as

$$DM(\hat{\alpha}_1)(\xi) = \int_{\Gamma_0} DM(\xi, \lambda) \hat{\alpha}_1(\lambda) d\lambda = \frac{1}{2i\pi} \int_{\Gamma_0} \frac{m(\lambda)}{\xi - \lambda} \hat{\alpha}_1(\lambda) d\lambda \quad (24)$$

where $m(\lambda) = \frac{1}{\zeta_0^0(\lambda)}$ and TM is also an integral operator defined as

$$TM(\hat{\alpha}_1)(\xi) = \int_{\Gamma_0} TM(\xi, \lambda) \hat{\alpha}_1(\lambda) d\lambda = \frac{1}{2i\pi} \int_{\Gamma_0} \frac{m(\lambda)}{\xi - \lambda \cos 2\varphi - |\sin 2\varphi| \zeta_0^0(\lambda)} \hat{\alpha}_1(\lambda) d\lambda \tag{25}$$

Note that the function TM can be expressed as

$$TM(\xi, \lambda) = \frac{1}{2i\pi} \frac{m(\lambda)}{\xi - T_0(\lambda)}, \tag{26}$$

where, applying the variable change $\lambda = \cos \theta$

$$T_0(\lambda = \cos \theta) = \lambda \cos \widetilde{2\varphi} + \sin \widetilde{2\varphi} \zeta_0^0(\lambda) = \cos(\theta + \widetilde{2\varphi}) \tag{27}$$

with

$$\widetilde{2\varphi} = \begin{cases} 2\varphi & \text{if } 0 < 2\varphi < \pi \\ 2\pi - 2\varphi & \text{if } \pi < 2\varphi < 2\pi \end{cases} \tag{28}$$

By using this angular variable, defined differently for wedge angles lower and higher than π , the description of the spectral functions method can be written the same way for wedge angles lower and higher than π , even if the final results (the diffraction coefficients) are different for wedge angles $\pi < 2\varphi < 2\pi$ and $2\pi - 2\varphi$. Indeed, the variable 2φ appears in all the resolution, whereas the variable $\widetilde{2\varphi}$ appears only in the definition of the function T_0 in (27) and of the domain Ω_0 in which T_0 operates, defined as

$$\Omega_0 = \{\xi \in \mathbb{C}, \xi = \cos \theta, 0 < \text{Re } \theta < \pi - \widetilde{2\varphi}\}. \tag{29}$$

Domain Ω_0 is delineated by the hyperbola

$$\partial\Omega_0^+ = \{\xi \in \mathbb{C}, \xi = \cos \theta, \text{Re } \theta = \pi - \widetilde{2\varphi}\}. \tag{30}$$

Domain Ω_0 and its upper boundary $\partial\Omega_0^+$ are illustrated on Fig. 3. Domain Ω_0 is the dotted area in Fig. 3. Arrows \mathcal{F}_1 and \mathcal{F}_2 on Fig. 3 are described later in section 3.2.

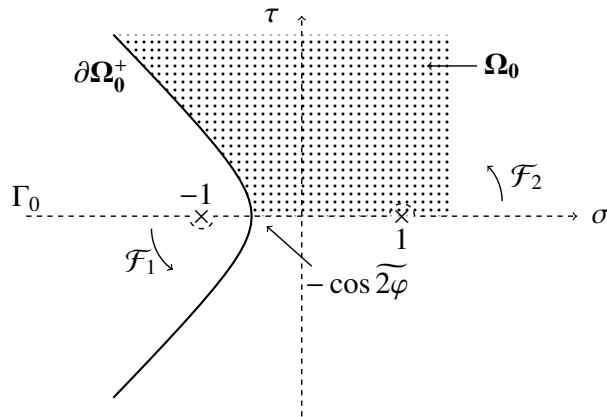


Fig. 3: Domain Ω_0 (the dotted area) and its upper boundary $\partial\Omega_0^+$. The lower boundary of Ω_0 is the semi-axis $[-\cos \widetilde{2\varphi}, +\infty[$. Arrows \mathcal{F}_1 and \mathcal{F}_2 show the deformation of Γ_0 (in thick dashed line) into $\partial\Omega_0^+$.

Having found the system of functional equations, it is now resolved following the methodology of [27].

3.2. System resolution

The resolution of the system of functional equations (23) is necessary in order to find the values of the spectral functions $\hat{\alpha}_1$ and $\hat{\alpha}_2$. With these values, the diffraction coefficients can be computed [see Eq. (92)].

It is shown in [27] that DM and TM integral operators are constituted of a "singular term" and of a "regular term". For a singular function

$$\phi(\xi) = \frac{1}{\xi - z}, \quad z \in \mathbb{C} \setminus]-\infty, -1] \text{ with } \text{Im } z \geq 0, \quad (31)$$

DM and TM integral operators defined respectively in (24) and (25) can be decomposed using the residue theorem as

$$DM(\phi)(\xi) = \int_{\Gamma_0} DM(\xi, \lambda) \cdot \frac{1}{\lambda - z} d\lambda = \frac{m(z)}{\xi - z} + D_p(\xi, z) \quad (32a)$$

$$TM(\phi)(\xi) = \int_{\Gamma_0} TM(\xi, \lambda) \cdot \frac{1}{\lambda - z} d\lambda = \frac{m(z)}{\xi - T_0(z)} \mathbf{1}(z \in \Omega_0) + T_p(\xi, z), \quad (32b)$$

where the function T_0 is defined in (27) and where

$$\mathbf{1}(z \in \Omega_0) = \begin{cases} 1 & \text{if } z \in \Omega_0, \\ 0 & \text{else} \end{cases} \quad (33)$$

and integrals D_p and T_p are holomorphic on $\mathbb{C} \setminus]-\infty, -1]$. Such integrals are expressed as

$$D_p(\xi, z) = \frac{1}{2\pi i} \int_{\Gamma_1} \frac{m(\lambda)}{\xi - \lambda} \cdot \frac{1}{\lambda - z} d\lambda, \quad (34a)$$

$$T_p(\xi, z) = \frac{1}{2\pi i} \int_{\partial\Omega_0^+} \frac{m(\lambda)}{\xi - T_0(\lambda)} \cdot \frac{1}{\lambda - z} d\lambda. \quad (34b)$$

Contours Γ_1 and $\partial\Omega_0^+$ are illustrated on Figs. 4 and 3 respectively.

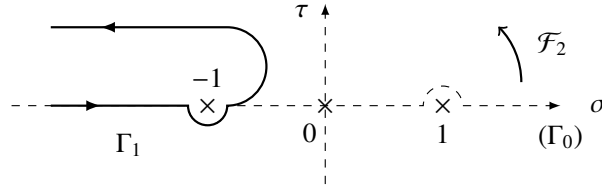


Fig. 4: Contour Γ_1 . Arrow \mathcal{F}_2 shows the deformation of Γ_0 (in dashed line) into Γ_1 .

In the sequel, using the decomposition of the DM and TM operators for a function of the form of (31), it will be shown that the unknown spectral functions $\hat{\alpha}_1$ and $\hat{\alpha}_2$ in the system (23) have a singular part. The first step for the resolution of the system (23) is then to determine this singular part.

3.2.1. Singular part

It is well known that poles of the spectral functions lead to the reflections of the incident field on the wedge faces (these reflections can be multiple), and to the fictitious fields that compensate the incident wave in the shadow zones. The sum of these reflections with the fictitious compensating fields constitute the aforementioned GE field. The singular part of the spectral functions contains these poles. The goal of this subsection is to calculate the poles and the corresponding residues and then to determine the expression of the singular part of the spectral functions, by employing a recursive algorithm.

Knowing the incident field on the wedge faces, the spectral function $\hat{\alpha}_j$ can be written as

$$\hat{\alpha}_j(\xi) = \frac{V_j}{\xi - Z_j} + X'_j(\xi), \quad j = 1, 2 \quad (35)$$

where Z_1, Z_2 are the initial poles, given in (23) with unknown residues V_1 and V_2 and the functions X'_j are unknown, $j = 1, 2$. From (32a), it is known that

$$DM(\hat{\alpha}_j)(\xi) = \frac{m(Z_j) \cdot V_j}{\xi - Z_j} + D_p(\xi, Z_j) \cdot V_j + DM(X'_j)(\xi). \quad (36)$$

By choosing $V_j = m^{-1}(Z_j)$, the right hand side of the system (23) is suppressed by the first term in the right hand side of (36). The resulting system's unknown functions are X'_j , $j = 1, 2$:

$$DM(X'_j)(\xi) + TM(X'_{3-j})(\xi) = -TM\left(\frac{V_{3-j}}{\xi - Z_{3-j}}\right)(\xi) - D_p(V_j, Z_j)(\xi) \quad j = 1, 2 \quad (37)$$

Besides, from (32b), we know that

$$TM\left(\frac{V_j}{\xi - Z_j}\right)(\xi) = \frac{m(Z_j) \cdot V_j}{\xi - T_0(Z_j)} \mathbf{1}(Z_j \in \Omega_0) + T_p(\xi, Z_j) \cdot V_j \quad j = 1, 2 \quad (38)$$

Thus, X'_j has a pole at $\xi = Z_j^2 = T_0(Z_{3-j})$ if $Z_{3-j} \in \Omega_0$. T_0 function defined in (27) is then called translation operator because it translates a pole of the spectral function $\hat{\alpha}_j$, $j = 1, 2$, to a pole of the spectral function $\hat{\alpha}_{3-j}$. The wave incident on face F_{3-j} is reflected. This reflected wave is incident on face F_j , generating a new pole $Z_j^2 = T_0(Z_{3-j})$. The unknown function X'_j in (35) is then decomposed as

$$X'_j(\xi) = \frac{V_j^2}{\xi - Z_j^2} + X''_j(\xi), \quad j = 1, 2 \quad (39)$$

where the function X''_j is unknown. Once again, the residues V_j^2 of these generated poles Z_j^2 are chosen so that they cancel the singular term $DM(X'_j)(\xi)$, found using the formula (32a), compensating the singular term in the TM operator in (38).

This pole propagation process is applied recursively in order to determine all the poles of the spectral functions $\hat{\alpha}_j$. This process stops when the generated poles are no longer in the domain Ω_0 defined in (29). All the generated poles then belong to $\Omega_0 \cup] -\cos 2\varphi, +\infty]$. Their imaginary part is then always positive due to the definition of the domain Ω_0 (see Fig. 3).

At the end of this process, spectral functions have the decomposition

$$\hat{\alpha}_j = Y_j + X_j, \quad (40)$$

where Y_j is the singular part, X_j is the regular part and $j = 1, 2$ is the face index. The singular part is expressed as

$$Y_j(\xi) = \sum_i \frac{V_j^i}{\xi - Z_j^i}, \quad (41)$$

where $i \in \mathbb{N}^*$, $Z_j^1 = Z_j$ defined in (23) is the initial pole on each face of the wedge,

$$Z_j^{i+1} = T_0(Z_k^i), \quad j, k \in \{1, 2\}, \quad k \neq j \quad (42)$$

are the different generated poles with their respective residue

$$V_j^{i+1} = -m^{-1}(T_0(Z_k^i)) m(Z_k^i) V_k^i \mathbf{1}(Z_k^i \in \Omega_0), \quad k \neq j. \quad (43)$$

. Figure 5 represents the generated poles in the complex plane for two different cases : figure 5a for a wedge of angle $\varphi = 80^\circ$ with an incident angle of $\theta_{inc} = 55^\circ$ and figure 5b for $\varphi = 20^\circ$ and $\theta_{inc} = 15^\circ$. As the wedge angle decreases, the number of poles increases, some poles being very close to one another, rendering the method less accurate for very small wedge angles.

The second step of the system resolution is the determination of the regular part X_j of the spectral function $\hat{\alpha}_j$ [see Eq. (40)]. The regular part is determined by using the Galerkin collocation method. Section 3.2.2 gives the principal steps of this resolution method.

3.2.2. Regular part

After the determination of the singular part of the solution using the pole propagation process explained in section 3.2.1, the remaining right hand side of (23) is composed of D_p and T_p functions. Thus, the system 23 becomes by construction

$$\begin{cases} DM(X_1)(\xi) + TM(X_2)(\xi) = -\sum_k (D_p(\xi, Z_1^k) \cdot V_1^k + T_p(\xi, Z_2^k) \cdot V_2^k) \\ TM(X_1)(\xi) + DM(X_2)(\xi) = -\sum_k (T_p(\xi, Z_1^k) \cdot V_1^k + D_p(\xi, Z_2^k) \cdot V_2^k) \end{cases} \quad (44)$$

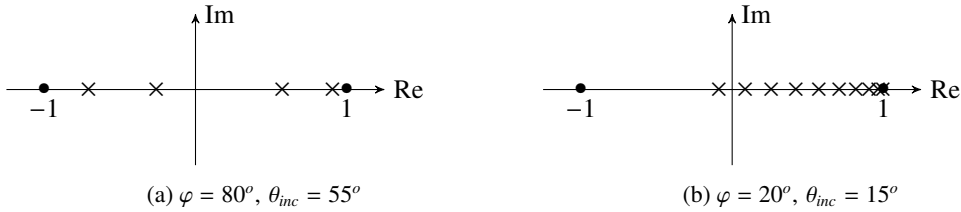


Fig. 5: Generated poles plotted in the complex plane

where X_j , $j = 1, 2$ are the regular parts of the spectral functions (40), D_p and T_p functions are defined in (34) and Z_j^k are the poles of the spectral function \hat{a}_j with their respective residue V_j^k . D_p and T_p are holomorphic functions on $\mathbb{C} \setminus]-\infty, -1]$ according to [27], and therefore the functions X_j are also holomorphic on this domain.

The functions $X_j(\xi)$, being holomorphic on $\mathbb{C} \setminus]-\infty, -1]$, can be approximated in the basis φ_k , $1 \leq k \leq N$ given by

$$\varphi_k(\xi) = \frac{d_k}{\xi + a_k}, \quad a_k \in [1, \infty[, \quad d_k = \sqrt{\frac{a_k}{\pi}}. \tag{45}$$

The discretization of the solution $X_j(\xi)$ in this finite basis is called a Galerkin approximation.

In the following, the integration contour Γ_0 pictured on Fig. 2 is deformed into the imaginary axis. If $f(\lambda)$ is a holomorphic function on $\mathbb{C} \setminus]-\infty, -1]$, the function $\tilde{f}(y) = f(iy)$ is introduced so that \tilde{f} is holomorphic on $\mathbb{C} \setminus i[1, \infty[$. The variable change $\lambda = iy$ gives a new basis

$$e_{a_k}(y) = \frac{d_k}{y - ia_k} = i\tilde{\varphi}(y), \quad \text{with } d_k = \sqrt{\frac{a_k}{\pi}} \quad \text{and } a_k \in [1, \infty[, \tag{46}$$

Having an approximation basis of the regular part of the spectral functions, $X_j(\xi)$ can be expressed as

$$X_j(\xi) \approx \sum_{k=1}^N \tilde{X}_j^k \varphi_k(\xi), \quad \tilde{X}_j^k \in \mathbb{C}. \tag{47}$$

The coordinates \tilde{X}_j^k are unknown. The system (44) then becomes, for $j = 1, 2$

$$\sum_{k=1}^N \left[\tilde{X}_j^k \int_{\Gamma_0} DM(\xi, \lambda) \varphi_k(\lambda) d\lambda + \tilde{X}_{3-j}^k \int_{\Gamma_0} TM(\xi, \lambda) \varphi_k(\lambda) d\lambda \right] = u_j(\xi), \tag{48}$$

where

$$u_j(\xi) = - \sum_k (D_p(\xi, Z_j^k) \cdot V_j^k + T_p(\xi, Z_{3-j}^k) \cdot V_{3-j}^k) \quad j = 1, 2 \tag{49}$$

The variable changes $\lambda = iy$ and $\xi = ix$ in (48) lead to the following system ($j = 1, 2$)

$$\sum_{k=1}^N \left[\tilde{X}_j^k \int_{-\infty}^{\infty} \widetilde{DM}(x, iy) e_{a_k}(y) dy + \tilde{X}_{3-j}^k \int_{-\infty}^{\infty} \widetilde{TM}(x, iy) e_{a_k}(y) dy \right] = \tilde{u}_j(x) \tag{50}$$

where $\widetilde{DM}(x, iy) = DM(ix, iy)$ and $\widetilde{TM}(x, iy) = TM(ix, iy)$. Following [27], we introduce another subspace of finite dimension in $L^2(\mathbb{R})$ which is generated by vectors e_{b_k} with

$$e_{b_k}(y) = \frac{d_k}{y - ib_k}, \quad \text{Re}(b_k) \in [1, \infty[\quad \text{and} \quad \text{Im}(b_k) = 0^-. \tag{51}$$

The b_k are called collocation points. The system (50) is projected in this subspace using the following relation :

$$(\tilde{\phi} | e_{b_k})_{L^2(\mathbb{R})} = (-2i\pi) d_k \phi(b_k) \tag{52}$$

Using (52), the projection of the system (50) leads to the following new systems (for $j = 1, 2$)

$$\begin{cases} \sum_{k=1}^N [\tilde{X}_j^k \int_{-\infty}^{\infty} DM(b_1, iy)e_{a_k}(y) dy + \tilde{X}_{3-j}^k \int_{-\infty}^{\infty} TM(b_1, iy)e_{a_k}(y) dy] = u_j(b_1) \\ \vdots \\ \sum_{k=1}^N [\tilde{X}_j^k \int_{-\infty}^{\infty} DM(b_N, iy)e_{a_k}(y) dy + \tilde{X}_{3-j}^k \int_{-\infty}^{\infty} TM(b_N, iy)e_{a_k}(y) dy] = u_j(b_N) \end{cases} \quad (53)$$

The obtained system (53) is a linear system of equations and can be put in a matrix format:

$$\begin{bmatrix} [D] & [T] \\ [T] & [D] \end{bmatrix} \begin{bmatrix} \bar{X}_1 \\ \bar{X}_2 \end{bmatrix} = \begin{bmatrix} U_1 \\ U_2 \end{bmatrix} \quad (54)$$

where

$$\bar{X}_j = \begin{bmatrix} \tilde{X}_j^1 \\ \vdots \\ \tilde{X}_j^N \end{bmatrix}, \tilde{X}_j^k \in \mathbb{C}; \quad U_j = \begin{bmatrix} u_j(b_1) \\ \vdots \\ u_j(b_N) \end{bmatrix}, u_j(b_k) \in \mathbb{C} \quad (55)$$

and

$$[D]_{lk} = \int_{-\infty}^{\infty} DM(b_l, iy)e_{a_k}(y) dy \quad (56)$$

$$[T]_{lk} = \int_{-\infty}^{\infty} TM(b_l, iy)e_{a_k}(y) dy \quad (57)$$

are the matrix elements of $[D]$ and $[T]$ respectively. System (54) can be rewritten as

$$\begin{cases} ([D] + [T]) (\bar{X}_1 + \bar{X}_2) = U_1 + U_2 \\ ([D] - [T]) (\bar{X}_1 - \bar{X}_2) = U_1 - U_2 \end{cases} \quad (58)$$

To find the regular part of the spectral functions (47), its coordinates \tilde{X}_j^k in the Galerkin basis φ_k , $1 \leq k \leq N$ defined in (45) must be determined. These coordinates are solutions of the linear system of equations (54) or (58). To resolve such a system, the matrices $[D]$ and $[T]$ and its right hand side $U_{1,2}$ must be calculated.

Matrices calculation

The first step is to determine $[D]$ and $[T]$ matrices. Using (24) and (46), the $[D]_{lk}$ elements defined in (56) can be expressed as

$$(-2i\pi)[D]_{lk} = -id_k \mathcal{D}(a_k, b_l) \quad (59)$$

with the function $\mathcal{D}(a, b)$ defined for $a > 1$ and $b > 1$ as

$$\mathcal{D}(a, b) = \int_{-\infty}^{+\infty} \frac{m(iy)}{y + ib} \frac{1}{y - ia} dy = \int_{-\infty}^{+\infty} \frac{1}{y + ib} \frac{1}{y - ia} \frac{1}{\zeta_0^0(iy)} dy. \quad (60)$$

Using (25) and (46) the $[T]_{lk}$ elements defined in (57) can be expressed as

$$(-2i\pi)[T]_{lk} = -d_k \mathcal{T}(a_k, b_l) \quad (61)$$

where the function $\mathcal{T}(a, b)$ is defined for $a > 1$ and $b > 1$ as

$$\mathcal{T}(a, b) = \int_{-\infty}^{+\infty} \frac{1}{b - iy \cos 2\varphi + |\sin 2\varphi| \sqrt{1 + y^2}} \frac{1}{y - ia} \frac{1}{\zeta_0^0(iy)} dy. \quad (62)$$

According to (16), $\mathcal{D}(a, b)$ and $\mathcal{T}(a, b)$ functions can be simplified using the relation

$$\zeta_0^0(iy) = -\sqrt{1 + y^2}. \quad (63)$$

The function $\mathcal{T}(a, b)$ is first calculated. The variable change

$$y = \frac{2x}{1-x^2}; \quad \frac{1+x^2}{1-x^2} = \sqrt{1+y^2}; \quad dy = 2 \frac{x^2+1}{(1-x^2)^2} dx \tag{64}$$

is applied to (62) :

$$\mathcal{T}(a, b) = 2 \int_{-1}^1 \frac{x^2 - 1}{b(1-x^2) - 2ix \cos 2\varphi + |\sin 2\varphi|(1+x^2)} \frac{1}{2x - ia(1-x^2)} dx \tag{65}$$

Let us define the polynomial functions $P(x)$ and $Q(x)$ as

$$P(x) = b(1-x^2) - 2ix \cos 2\varphi + |\sin 2\varphi|(1+x^2), \tag{66}$$

$$Q(x) = 2x - ia(1-x^2). \tag{67}$$

The integrand of the $\mathcal{T}(a, b)$ function (65) is a rational function which can be decomposed in the partial fraction :

$$\frac{-1+x^2}{PQ} = \frac{\gamma x + \delta}{P} + \frac{\alpha x + \beta}{Q} \tag{68}$$

as long as $\Delta \neq 0$, with

$$\Delta = a^2 + b^2 + 2ab \cos \varphi - (\sin \varphi)^2 \neq 0 \tag{69}$$

Using this partial fraction decomposition, $\mathcal{T}(a, b)$ function (65) can be written as

$$\mathcal{T}(a, b) = 2 \int_{-1}^1 \left(\frac{\gamma x + \delta}{P(x)} + \frac{\alpha x + \beta}{Q(x)} \right) dx, \tag{70}$$

It is shown in appendix Appendix A that

$$\int_{-1}^1 \frac{\alpha x + \beta}{Q(x)} dx = \alpha \text{sog}(a) + i\beta \text{rog}(a) \tag{71}$$

and that

$$\int_{-1}^1 \frac{\gamma x + \delta}{P(x)} dx = \frac{i\gamma}{b - \sin 2\varphi} \left[\left(\frac{\pi}{2} - 2\varphi \right) - \cos 2\varphi \text{rog}(b) \right] + \delta \text{rog}(b). \tag{72}$$

where rog and sog are defined in appendix Appendix A. Finally, using (71), (72) and (70),

$$\mathcal{T}(a, b) = 2 [T_1(a, b) + T_2(a, b)] \tag{73}$$

with

$$T_1(a, b) = \alpha \text{sog}(a) + i\beta \text{rog}(a), \tag{74a}$$

$$T_2(a, b) = \frac{i\gamma}{b - \sin 2\varphi} \left[\left(\frac{\pi}{2} - 2\varphi \right) - \cos 2\varphi \text{rog}(b) \right] + \delta \text{rog}(b). \tag{74b}$$

Integral $\mathcal{D}(a, b)$ given in (60) can then be rewritten, using a partial fraction decomposition, as

$$\mathcal{D}(a, b) = \frac{i}{b+a} \int_{-\infty}^{+\infty} \left(\frac{1}{y-ia} \frac{1}{\sqrt{1+y^2}} - \frac{1}{y+ib} \frac{1}{\sqrt{1+y^2}} \right) dy, \quad \text{if } a+b \neq 0. \tag{75}$$

Using the variable change (64), we have for $a \geq 1$,

$$\int_{\mathbb{R}} \frac{1}{y-ia} \frac{1}{\sqrt{1+y^2}} dy = 2i \int_{-1}^1 \frac{1}{a(1-x^2) + 2ix} dx = 2i \text{rog}(a) \tag{76}$$

and for $b \geq 1$

$$\int_{\mathbb{R}} \frac{1}{y+ib} \frac{1}{\sqrt{1+y^2}} dy = \overline{\int_{\mathbb{R}} \frac{1}{y-ib} \frac{1}{\sqrt{1+y^2}} dy} = \overline{2i \operatorname{rog}(b)} = -2i \operatorname{rog}(b). \tag{77}$$

From (76) and (77), Eq. (75) reduces to

$$\mathcal{D}(a, b) = \frac{-2}{a+b} [\operatorname{rog}(a) + \operatorname{rog}(b)]. \tag{78}$$

The matrices $[D]$ and $[T]$ are now completely determined using (59) and (61) respectively. Their analytical properties are also known. In order to resolve the linear system of equations (54) or (58), their right hand side constituted of U_1 and U_2 must also be computed.

Determination of the right hand side of the system of equations

Using (49), the right hand side of the system (53) which is calculated at the collocation points b_l defined in (51), $l \in \{1, 2, \dots, N\}$, is

$$u_j(b_l) = - \sum_k \left(D_p(b_l, Z_j^k) \cdot V_j^k + T_p(b_l, Z_{3-j}^k) \cdot V_{3-j}^k \right) \quad j = 1, 2 \tag{79}$$

where D_p and T_p functions are defined in (32) and Z_j^k is defined in (42), $k \in \mathbb{N}^*$.

Taking the definition of the D_p function in (32a), and deforming the contour Γ_0 pictured on Fig. 2 into the imaginary axis by applying the variable change $\lambda = iy$, we get

$$D_p(b_l, z) = \frac{1}{2\pi} \mathcal{D}(-z, b_l) - \frac{m(z)}{b_l - z}. \tag{80}$$

Similarly, using the definition of the T_p function given in (32b), and by deforming the integrand contour Γ_0 pictured on Fig. 2 into the imaginary axis by applying the variable change $\lambda = iy$ we have

$$T_p(b_l, z) = \frac{1}{2i\pi} \mathcal{T}(-z, b_l) - \frac{m(z)}{b_l - T_0(z)} \mathbf{1}(z \in \Omega_0). \tag{81}$$

Expressions (80) of D_p and (81) of T_p functions are incorporated in the right hand side of the system (79) with $z = Z_j^k$ for each $u_j(b_l)$, $j = 1, 2$. In this new expression, with the pole propagation process explained in section 3.2.1, singular terms of D_p and T_p functions cancel each other. The remaining term in the right hand side of the system (79) is therefore, for $j = 1, 2$; $l \in \{1, 2, \dots, N\}$

$$(2\pi i) u_j(b_l) = - \sum_k \left(i \mathcal{D}(-Z_j^k, b_l) \cdot V_j^k + \mathcal{T}(-Z_{3-j}^k, b_l) \cdot V_{3-j}^k \right) + \frac{2\pi i}{b_l - Z_j} \tag{82}$$

Once all matrix terms have been calculated, system (54) is resolved numerically. For that, the NAG numeric subroutine library for Fortran is used. With the resolution of this linear system of equations, the coordinates \tilde{X}_j^k of the regular term X_j of the spectral functions are known and therefore the regular term X_j is approximated using (47). The spectral functions $\hat{\alpha}_j$ are then completely determined using (40), (41) and (47).

3.3. Propagation of the solution

The regular part approximation described previously is not accurate in the entire complex plane. There exists a procedure, called "propagation of the solution" and explained in [27], which allows to propagate the accuracy of the regular part $X_j(\xi)$ of the spectral functions from $\xi \notin \Omega_0^-, \operatorname{Im}(\xi) < 0$ where the approximation is valid to the domain Ω_0^- where it is not. The space Ω_0^- defined by

$$\Omega_0^- = \{ \xi \in \mathbb{C}, \operatorname{Im}(\xi) < 0, \xi = \cos(\theta), \widetilde{2\varphi} < \operatorname{Re}(\theta) < \pi \} \tag{83}$$

is represented in Fig. 7. The procedure consists in deriving new recursive equations by deforming the contour Γ_0 in the integrals of the right-hand side of (44) into a new contour Γ_2 and taking into account the poles crossed in the process.

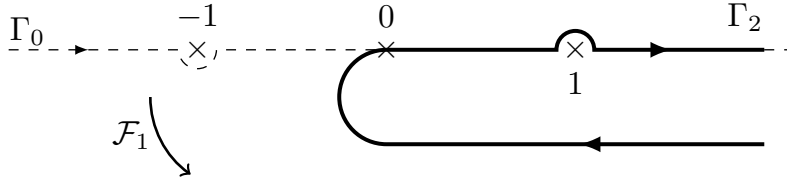


Fig. 6: Contour Γ_2 . Arrow \mathcal{F}_1 shows the deformation of Γ_0 into Γ_2 .

To begin, the contour Γ_0 in the DM integral operator is deformed into Γ_2 . The half-space $\{\lambda, \text{Im } \lambda < 0\}$ is then crossed during this contour deformation as shown by the F_1 arrow on Fig. 6.

During this contour deformation, only the poles

$$\lambda = \xi, \quad \text{with } \text{Im}(\xi) < 0 \tag{84}$$

of the DM function (24) are crossed and therefore, applying the residue theorem, we have for $\xi \in \mathbb{C}, \text{Im}(\xi) < 0, j = 1, 2,$

$$DM(X_j)(\xi) = \int_{\Gamma_0} DM(\xi, \lambda) X_j(\lambda) d\lambda = \int_{\Gamma_2} DM(\xi, \lambda) X_j(\lambda) d\lambda + m(\xi) X_j(\xi). \tag{85}$$

The poles of the TM function (25) are

$$\lambda = T_0^{-1}(\xi) = \xi \cos \widetilde{2\varphi} - \sin \widetilde{2\varphi} \zeta_0(\xi) = \cos(\theta - \widetilde{2\varphi}) \quad \text{if } \xi = \cos \theta$$

T_0^{-1} operates in the domain Ω_0^- , therefore they are crossed during this contour deformation if and only if $\xi \in \Omega_0^-$ (see dotted area on Fig. 7). The domain Ω_0^- is delineated by the hyperbola

$$\partial\Omega_0^- = \{\xi \in \mathbb{C}, \text{Im}(\xi) < 0, \xi = \cos \theta, \text{Re } \theta = \widetilde{2\varphi}\}. \tag{86}$$

Domain Ω_0^- and contour $\partial\Omega_0^-$ are illustrated on Fig. 7.

Applying the residue theorem to the TM integral operator then gives for $\xi \in \mathbb{C}, \text{Im}(\xi) < 0, j = 1, 2,$

$$TM(X_j)(\xi) = \int_{\Gamma_0} TM(\xi, \lambda) X_j(\lambda) d\lambda = \int_{\Gamma_2} TM(\xi, \lambda) X_j(\lambda) d\lambda + m(\xi) X_j[T_0^{-1}(\xi)] \mathbf{1}(\xi \in \Omega_0^-) \tag{87}$$

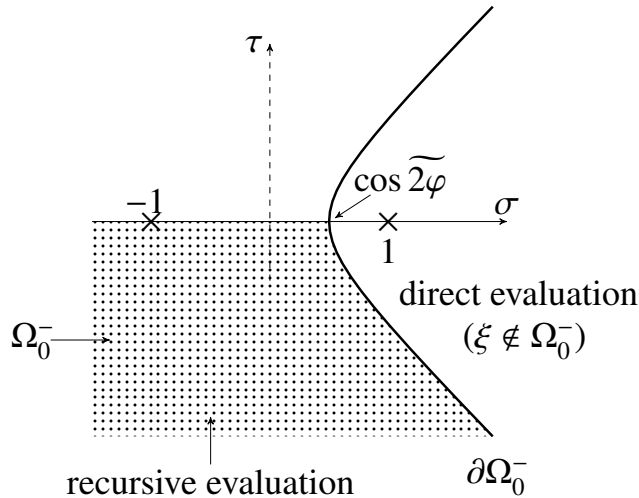


Fig. 7: Domain Ω_0^- and its lower boundary $\partial\Omega_0^-$ in the complex plane $\xi = \sigma + i\tau$. Ω_0^- is delimited by $\partial\Omega_0^-$ and the semi-axis $]-\infty, \cos \widetilde{2\varphi}]$.

Using (85) and (87) in the system of functional equations (44), the system (44) is then equivalent to this new system for $\xi \in \mathbb{C}, \text{Im}(\xi) < 0$:

$$\begin{cases} X_1(\xi) = g_1(\xi) - X_2(T_0^{-1}(\xi)) \mathbf{1}(\xi \in \Omega_0^-) \\ X_2(\xi) = g_2(\xi) - X_1(T_0^{-1}(\xi)) \mathbf{1}(\xi \in \Omega_0^-) \end{cases} \tag{88}$$

where

$$g_j(\xi) = m(\xi)^{-1} \left[u_j(\xi) - \int_{\Gamma_2} DM(\xi, \lambda) X_j(\lambda) d\lambda - \int_{\Gamma_2} TM(\xi, \lambda) X_{3-j}(\lambda) d\lambda \right] \tag{89}$$

Formula (88) is called the recursive formula because it uses the value of the regular function X_2 at point $T_0^{-1}(\xi)$ to compute the value of X_1 at the point ξ where the approximation is not valid (and vice-versa). If the translation from ξ to $T_0^{-1}(\xi)$ is not sufficient to reach the domain $\mathbb{C} \setminus \Omega_0^-$ where the approximation is valid, then the use of the formula is repeated as many times as necessary (computing $X_2(T_0^{-1}(\xi))$ using the value of $X_1(T_0^{-2}(\xi))$, etc.).

To calculate g_j functions, we need to compute

$$\int_{\Gamma_2} DM(\xi, \lambda) X_j(\lambda) d\lambda = \sum_k \tilde{X}_j^k \int_{\Gamma_2} DM(\xi, \lambda) \varphi_k(\lambda) d\lambda$$

and

$$\int_{\Gamma_2} TM(\xi, \lambda) X_j(\lambda) d\lambda = \sum_k \tilde{X}_j^k \int_{\Gamma_2} TM(\xi, \lambda) \varphi_k(\lambda) d\lambda$$

If $\text{Im}(a) < 0$, the residue theorem combined with the variable change $\lambda = iy$ yields

$$\int_{\Gamma_2} DM(\xi, \lambda) \frac{1}{\lambda + a} d\lambda = \frac{1}{2\pi} \mathcal{D}(a, \xi) - \frac{m(\xi)}{\xi + a} = \mathcal{N}\mathcal{D}(a, \xi). \tag{90}$$

For the TM contributions, the poles $\lambda = T_0^{-1}(\xi)$ are taken into account if and only if $\xi \in \Omega_0^-$. Thus, for $\xi \in \Omega_0^-$, $\text{Im}(a) < 0$, the residue theorem combined with the variable change $\lambda = iy$ gives

$$\int_{\Gamma_2} TM(\xi, \lambda) \frac{1}{\lambda + a} d\lambda = \frac{1}{2i\pi} \mathcal{T}(a, \xi) - \frac{m(\xi)}{T_0^{-1}(\xi) + a} = \mathcal{N}\mathcal{T}(a, \xi) \tag{91}$$

Formula (47) finally leads to, for $\xi \in \Omega_0^-$ and $j = 1, 2$,

$$m(\xi) g_j(\xi) - u_j(\xi) = - \left(\sum_k \tilde{X}_j^k d_k \mathcal{N}\mathcal{D}(a_k, \xi) + \sum_k \tilde{X}_{3-j}^k d_k \mathcal{N}\mathcal{T}(a_k, \xi) \right)$$

Some numerical results are presented in the sequel.

4. Numerical results

In this section, a far-field ($k_0 r \gg 1$) asymptotic evaluation of the diffraction coefficient is computed using the stationary phase method :

$$D(\theta) = \frac{e^{-i\frac{\pi}{4}}}{\sqrt{2\pi}} [\hat{\alpha}_1(-\cos \theta) + \hat{\alpha}_2(-\cos(2\varphi - \theta))] \tag{92}$$

where $\hat{\alpha}_1$ and $\hat{\alpha}_2$ are the spectral functions, is compared to the analytic expression of the diffraction coefficient of the scattering of a plane wave with a wedge at interfaces fluid/void as expressed by Sommerfeld [1]. Keller [4] gives an analytical expression of the GTD approximation of the coefficient in the case of the diffraction of a scalar plane wave by a wedge with Dirichlet boundaries which can be used in the case of a stress-free wedge immersed in a fluid :

$$D^{(\text{Dir})}(\theta) = \frac{e^{i\frac{\pi}{4}}}{2N\sqrt{2\pi}} \left[\cot\left(\frac{\pi + (\theta + \theta_{\text{inc}})}{2N}\right) + \cot\left(\frac{\pi - (\theta + \theta_{\text{inc}})}{2N}\right) - \cot\left(\frac{\pi + (\theta - \theta_{\text{inc}})}{2N}\right) - \cot\left(\frac{\pi - (\theta - \theta_{\text{inc}})}{2N}\right) \right], \tag{93}$$

with $N = 2\varphi/\pi$.

To apply the recursive procedure described in 3.3, calculation points ξ must have a negative imaginary part. The calculation points considered are then

$$\xi_1 = -\cos \theta - i 10^{-3} \quad \text{and} \quad \xi_2 = -\cos(2\varphi - \theta) - i 10^{-3}, \tag{94}$$

where θ is the observation angle in the wedge (see Fig. 1).

For the Galerkin basis defined in (46), the parameters $a_k \in [1, \infty[$ are chosen as an exponential law [27]:

$$\begin{aligned} a_k &= 1.1 + 0.05 \left(10^{\frac{k-1}{4}} - 1 \right), \quad 1 \leq k \leq 20 \\ b_k &= a_k - i0.1, \quad 1 \leq k \leq 20. \end{aligned} \tag{95}$$

The module of the diffraction coefficients computed using spectral functions and Sommerfeld integral method for various wedge angles are plotted in terms of the observation angle θ , $0 \leq \theta \leq 2\varphi$ and presented on Fig. 8.

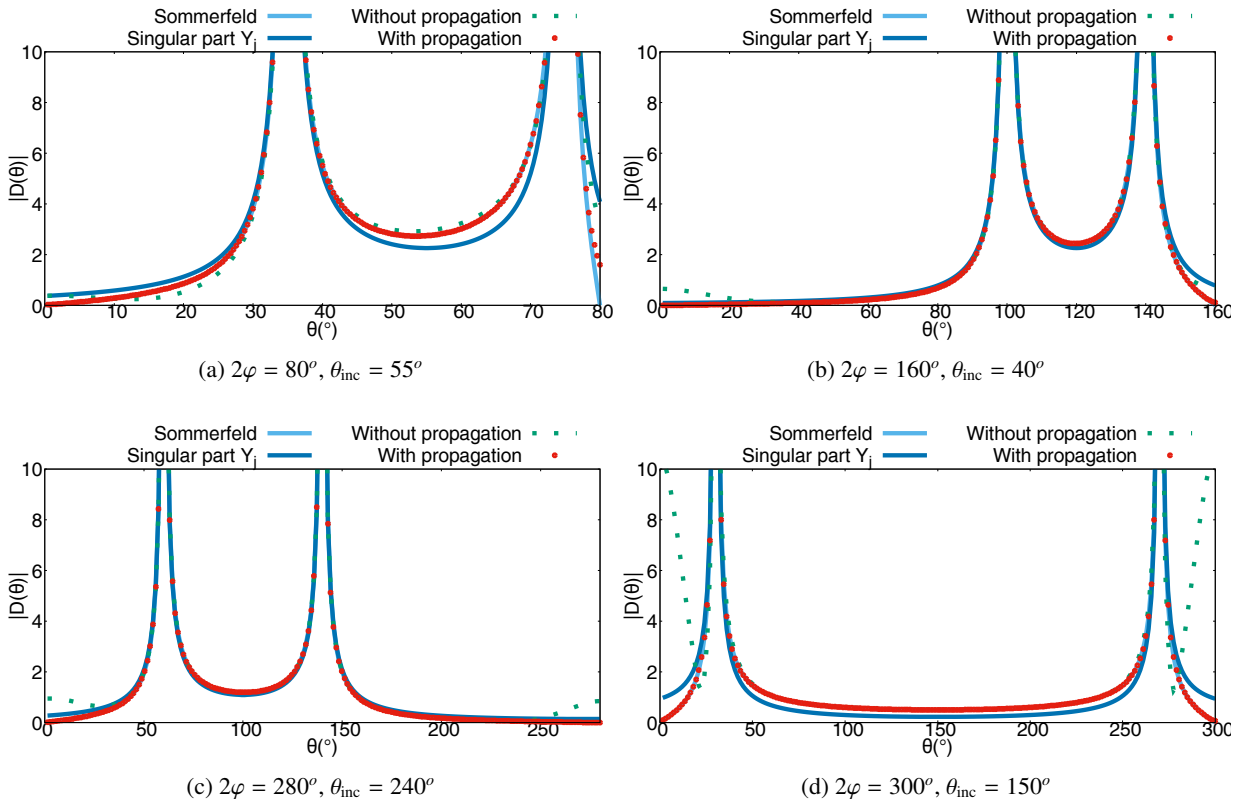


Fig. 8: Diffraction coefficient computed with the spectral functions and with the Sommerfeld method, in the case of Dirichlet boundary conditions.

In the case of Neumann boundary conditions, the initial system (7) is replaced by the following :

$$\begin{cases} (\Delta + 1)v = 0 & \text{in } \Omega_f, \\ \partial v / \partial n = -\partial h_{inc} / \partial n & \text{on } F_j, \quad j = 1, 2 \end{cases}, \tag{96}$$

where n is the inward-pointing normal to the wedge faces. The spectral functions method can once again be applied following the same steps as for the Dirichlet boundary conditions. The details of the computation are not repeated here. Once again, a far-field evaluation of the diffraction, given by (92) is compared to the analytic expression of the diffraction coefficient given by Sommerfeld [1]. The GTD approximation of this coefficient is also given by Keller

[4] :

$$D^{(\text{New})}(\theta) = \frac{e^{i\frac{\pi}{4}}}{2N\sqrt{2\pi}} \left[\cot\left(\frac{\pi + (\theta + \theta_{\text{inc}})}{2N}\right) + \cot\left(\frac{\pi - (\theta + \theta_{\text{inc}})}{2N}\right) \right. \\ \left. + \cot\left(\frac{\pi + (\theta - \theta_{\text{inc}})}{2N}\right) + \cot\left(\frac{\pi - (\theta - \theta_{\text{inc}})}{2N}\right) \right] \quad (97)$$

with $N = 2\varphi/\pi$. The results are presented on Fig 9.

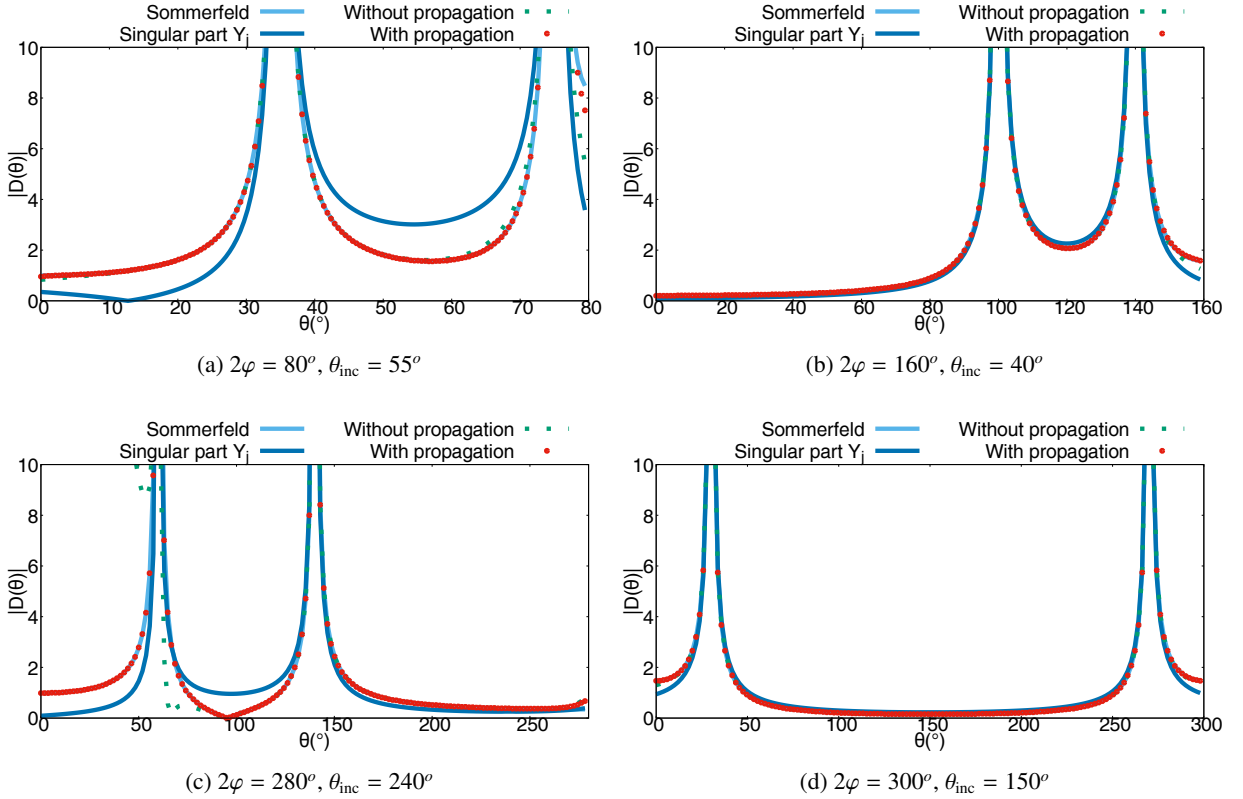


Fig. 9: Diffraction coefficient computed with the spectral functions and with the Sommerfeld method, in the case of Neumann boundary conditions.

In each of these figures, the continuous light blue line represents the modules of the diffraction coefficients obtained using the Sommerfeld integral method, the continuous dark blue line represents those obtained using the Spectral function singular part Y_j alone, the short-dashed green line represents those obtained using the Spectral functions method without propagation of the solution and the red circles represent those obtained using the spectral functions method with propagation of the solution described in paragraph 3.3.

On Figs. 8a, 8b, 9a and 9b the wedge angles are lower than π and on figs. 8d, 8c, 9d and 9c the wedge angles are greater than π . In all cases, it appears clearly that both the regular part of the solution and the recursive method are necessary to obtain optimal results. When both of these are included, diffraction coefficients obtained with Spectral functions are close to those of the Sommerfeld method. In addition, the run time to evaluate the diffraction coefficients in 250 different observation points, in each of the presented configurations, using an Intel(R) Xeon(R) CPU E3-1240 v3 is under 0.1 seconds for both methods.

5. Conclusion

The spectral functions method is shown here to model diffraction of an acoustic wave from stress-free wedges. The diffraction coefficient obtained using the spectral functions has been compared to the analytic one obtained from the asymptotic evaluation of the Sommerfeld integral. The numerical results obtained thanks to the spectral

functions method are very close to those given by the analytical solution and a precise result is obtained at a very low computational cost. The acoustic wave diffraction by a wedge with Neumann boundary conditions has also been modeled and successfully validated. The spectral functions method may be extended to more complex wedge diffraction cases such as elastic wave diffraction. In these cases, studies may be carried out to numerically calculate corresponding diffraction coefficients for all wedge angles with a good precision and a low computation time.

Appendix A. Calculation details of integrals in section 3.2.2

Appendix A.1. Definition of rog and sog complex functions

Let us introduce $\text{rog}(a)$ and $\text{sog}(a)$ complex functions defined as

$$\text{rog}(a) = \int_{-1}^1 \frac{1}{a(1-x^2) + 2ix} dx, \quad (\text{A.1})$$

$$\text{sog}(a) = \frac{1}{a} \left(\frac{\pi}{2} - \text{rog}(a) \right) \quad (\text{A.2})$$

These functions are used in the sequel to express $\mathcal{T}(a, b)$ [see Eq. (70)] and $\mathcal{D}(a, b)$ [see Eq. (60)] functions. Their analytic properties are given hereafter.

Lemma Appendix A.1. *The function $\text{rog}(a)$ defined for $a > 1$ by*

$$\text{rog}(a) = \int_{-1}^1 \frac{1}{a(1-x^2) + 2ix} dx$$

is holomorphic on $\mathbb{C} \setminus \{-1\}$ and has the following property :

For $x \neq \pm 1$,

$$\text{rog}(a) = \frac{1}{\sqrt{a^2 - 1}} \ln(a + \sqrt{a^2 - 1}) \quad (\text{A.3})$$

Proof The roots of the polynomial $a(1-x^2) + 2ix$, $a \in \mathbb{C}^*$ are $x_{\pm} = \frac{1}{a}(i \pm \sqrt{a^2 - 1})$. When $a \notin \{-1, 0, 1\}$, these roots are distinct and formula (A.3) results from a classical integral computation. When $a = 0$, both formulations (A.1) and (A.3) give $\text{rog}(0) = \frac{\pi}{2}$ and no singularity arises. However, when $a = 1$, (A.1) yields $\text{rog}(1) = 1$ whereas (A.3) presents a singularity. The indetermination is lifted by defining $z = \sqrt{1 - 1/a^2}$ in (A.3). We then have :

$$\text{rog}(a) = \frac{1}{2az} \ln \left(\frac{1+z}{1-z} \right) \quad (\text{A.4})$$

The Taylor series expansion at $z = 0$ leads to $\text{rog}(1) = 1$. The rog function can therefore be extended to $\mathbb{C} \setminus \{-1\}$.

Lemma Appendix A.2. *The function $\text{sog}(x)$ defined in (A.2) for $x > 1$ is holomorphic on $\mathbb{C} \setminus \{-1\}$.*

Proof sog function defined in (A.2) depends on the rog function which is holomorphic on $\mathbb{C} \setminus \{-\infty, -1\}$. To remove the indetermination near $x = 0$, let us define $y = (1 - x^2)^{1/2}$. We then have $x = -i(y^2 - 1)^{1/2}$ using the same definition of the square root as in (16b). Thus,

$$\text{sog}(x) = -\frac{\pi}{2} \frac{x}{y(y+1)} + \frac{1}{y} \text{rog}(y) \quad \text{with } y \rightarrow 1 \quad (\text{A.5})$$

Knowing the analytic properties of functions rog and sog , we can now calculate the integrals $\mathcal{T}(a, b)$ (70) and $\mathcal{D}(a, b)$ (60).

Appendix A.2. Partial fractions integration

Integrals to calculate in the subsection "matrix calculation" of section 3.2.2 are in the following form:

$$I_1 = \int_{-1}^1 \frac{\alpha x + \beta}{Q(x)} dx \quad (\text{A.6})$$

and

$$I_2 = \int_{-1}^1 \frac{\gamma x + \delta}{P(x)} dx \quad (\text{A.7})$$

with polynomial functions $P(x)$ and $Q(x)$ defined in (66) and (67) respectively.

Let us first calculate integral I_1 .

$$\begin{aligned} I_1 &= \int_{-1}^1 \frac{\alpha x + \beta}{iax^2 + 2x - ia} dx \\ &= \frac{\alpha}{2ia} \int_{-1}^1 \frac{2(iax + 1)}{iax^2 + 2x - ia} dx + \int_{-1}^1 \frac{\beta - \frac{\alpha}{ia}}{iax^2 + 2x - ia} dx \\ &= \frac{\pi\alpha}{2a} + \left(\frac{\beta}{ia} + \frac{\alpha}{a^2} \right) \int_{-1}^1 \frac{1}{x^2 + \frac{2}{ia}x - 1} dx \\ I_1 &= \alpha \operatorname{sog}(a) + i\beta \operatorname{rog}(a) \end{aligned} \quad (\text{A.8})$$

with rog and sog functions being defined in (A.1) and (A.2) respectively.

Now let us calculate integral I_2 , supposing $b \neq |\sin 2\varphi|$.

$$\begin{aligned} I_2 &= \int_{-1}^1 \frac{\gamma x + \delta}{b(1-x^2) - 2ix \cos 2\varphi + |\sin 2\varphi|(1+x^2)} dx \\ &= \frac{1}{2(|\sin 2\varphi| - b)} \int_{-1}^1 \frac{2\gamma \left[(|\sin 2\varphi| - b)x - i \cos 2\varphi \right] + 2 \left[i\gamma \cos 2\varphi + \delta (|\sin 2\varphi| - b) \right]}{x^2(|\sin 2\varphi| - b) - 2ix \cos 2\varphi + (b + |\sin 2\varphi|)} dx \\ &= \frac{i\gamma}{|\sin 2\varphi| - b} \left(\widetilde{2\varphi} - \frac{\pi}{2} \right) + \frac{1}{|\sin 2\varphi| - b} \left(\delta + \gamma \frac{i \cos 2\varphi}{|\sin 2\varphi| - b} \right) I_3 \end{aligned}$$

where

$$I_3 = \int_{-1}^1 \frac{1}{\left(x - \frac{i \cos \varphi}{|\sin 2\varphi| - b} \right)^2 - \frac{b^2 - 1}{(|\sin 2\varphi| - b)^2}} dt. \quad (\text{A.9})$$

We need to determine I_3 to access the value of I_2 .

$$\begin{aligned} I_3 &= \int_{-1}^1 \frac{1}{\left(x - \frac{i \cos \varphi}{|\sin 2\varphi| - b} - \frac{\sqrt{b^2 - 1}}{|\sin 2\varphi| - b} \right) \left(x - \frac{i \cos \varphi}{|\sin 2\varphi| - b} + \frac{\sqrt{b^2 - 1}}{|\sin 2\varphi| - b} \right)} dx \\ &= \frac{|\sin 2\varphi| - b}{\sqrt{b^2 - 1}} \ln \left(b + \sqrt{b^2 - 1} \right) \\ &= (|\sin 2\varphi| - b) \operatorname{rog}(b). \end{aligned} \quad (\text{A.10})$$

Finally, using (A.10) in (A.9),

$$I_2 = \frac{i\gamma}{|\sin 2\varphi| - b} \left(\widetilde{2\varphi} - \frac{\pi}{2} + i\gamma \cos 2\varphi \operatorname{rog}(b) \right) + \delta \operatorname{rog}(b). \quad (\text{A.11})$$

Acknowledgments

We would like to thank Lucien Rochery for his help computing and implementing the diffraction coefficient in the case of Neumann boundary conditions.

Competing interests

We have no competing interests.

Funding Source

This research did not receive any specific grant from funding agencies in the public, commercial, or not-for-profit sectors.

References

- [1] S. A., Asymptotische darstellung von formeln aus beugungstheorie des lichts, *Journal für die reine und angewandte Mathematik*. 158 (1928) 199–208.
- [2] G. V. Babich VM, Lyalinov MA, *Diffraction theory: Sommerfeld-Malyuzhinets technique.*, Alpha Science, 2008.
- [3] M. HM., *Electric waves : being an Adams prize essay in the University of Cambridge.*, Cambridge, 1902. URL: <http://hdl.handle.net/2027/hvd.32044080810880>.
- [4] J. B. Keller, Geometrical theory of diffraction*, *J. Opt. Soc. Am.* 52 (1962) 116–130.
- [5] R. G. Kouyoumjian, P. H. Pathak, A uniform geometrical theory of diffraction for an edge in a perfectly conducting surface, *Proceedings of the IEEE* 62 (1974) 1448–1461.
- [6] D. Bouche, F. Molinet, R. Mittra, *Asymptotic Methods in Electromagnetics*, Springer, 1997.
- [7] B. Lu, M. Darmon, L. Fradkin, C. Potel, Numerical comparison of acoustic wedge models, with application to ultrasonic telemetry, *Ultrasonics* 65 (2016) 5 – 9.
- [8] B. V. Budaev, D. B. Bogy, Rayleigh wave scattering by a wedge, *Wave Motion* 22 (1995) 239 – 257.
- [9] V. V. Kamotski, L. J. Fradkin, B. A. Samokish, V. A. Borovikov, V. M. Babich, On budaev and bogys approach to diffraction by the 2d tractionfree elastic wedge, *SIAM Journal on Applied Mathematics* 67 (2006) 235–259.
- [10] A. K. Gautesen, L. Fradkin, Diffraction by a two-dimensional traction-free elastic wedge, *SIAM Journal of Applied Mathematics* 70 (2010) 3065–3085.
- [11] A. K. Gautesen, Scattering of a Rayleigh wave by an elastic wedge whose angle is less than 180, *Wave Motion* 36 (2002) 417–424.
- [12] A. K. Gautesen, Scattering of a Rayleigh wave by an elastic wedge whose angle is greater than 180 degrees, *Journal of Applied Mechanics* 68 (2000) 476–479.
- [13] P. Ufimtsev, *Fundamentals of the Physical Theory of Diffraction.*, John Wiley & Sons, 2007.
- [14] V. Zernov, L. Fradkin, M. Darmon, A refinement of the kirchhoff approximation to the scattered elastic fields, *Ultrasonics* 52 (2012) 830 – 835.
- [15] R. Lewis, J. Boersma, Uniform asymptotic theory of edge diffraction, *Journal of Mathematical Physics* 10 (1969) 2291–2305.
- [16] J. D. Achenbach, A. K. Gautesen, H. McMaken, *Ray methods for waves in elastic solids: with applications to scattering by cracks* (1982).
- [17] F. Molinet, *Acoustic high-frequency diffraction theory*, New York: Momentum Press, 2011.
- [18] P. C. Clemmow, Some extensions to the method of integration by steepest descents, *The Quarterly Journal of Mechanics and Applied Mathematics* 3 (1950) 241–256.
- [19] A. Kamta Djakou, M. Darmon, L. Fradkin, C. Potel, The uniform geometrical theory of diffraction for elastodynamics: Plane wave scattering from a half-plane, *The Journal of the Acoustical Society of America* 138 (2015) 3272–3281.
- [20] V. H. Aristizabal, F. J. Velez, J. D. Jaramillo, Efficient solution for the diffraction of elastic sh waves by a wedge: Performance of various exact, asymptotic and simplified solutions, *Soil Dynamics and Earthquake Engineering* 95 (2017) 9 – 16.
- [21] S. Osher, Initial-boundary value problems for hyperbolic systems in regions with corners. i, *Transactions of the American mathematical society* 176 (1973) 141–165.
- [22] S. Osher, Initial-boundary value problems for hyperbolic systems in regions with corners. ii, *Transactions of the American mathematical society* 198 (1974) 155–175.
- [23] A. Huang, R. Temam, The linear hyperbolic initial and boundary value problems in a domain with corners, *Discrete and Continuous Dynamical Systems - Series B* 19 (2014) 1627–1665.
- [24] F. G. Friedlander, *Sound Pulses*, Cambridge Monographs on Mechanics and Applied Mathematics, 1958.
- [25] L. Castro, D. Kapanadze, Wave diffraction by wedges having arbitrary aperture angle, *Journal of Mathematical Analysis and Applications* 421 (2015) 1295 – 1314.
- [26] V. V. Kamotski, G. Lebeau, Diffraction by an elastic wedge with stress-free boundary: existence and uniqueness, *Proceedings of the Royal Society of London A: Mathematical, Physical and Engineering Sciences* 462 (2006) 289–317.
- [27] J.-P. Croisille, G. Lebeau, *Diffraction by an Immersed Elastic Wedge*, volume 1723, Springer, 2000.
- [28] K. Klem-Musatov, *Theory of seismic diffractions*, Society of Exploration Geophysicists, 1994.
- [29] A. M. Aizenberg, A. A. Ayzenberg, Feasible fundamental solution of the multiphysics wave equation in inhomogeneous domains of complex shape, *Wave Motion* 53 (2015) 66 – 79.
- [30] A. A. Ayzenberg, *Transmission-propagation operator theory and tip-wave superposition method for sub-salt shadow wavefield description*, Ph.D. thesis, Norwegian University of Science and Technology, 2015.